The role of autophagy during carbon starvation in Aspergillus niger

Burggraaf, M.A.

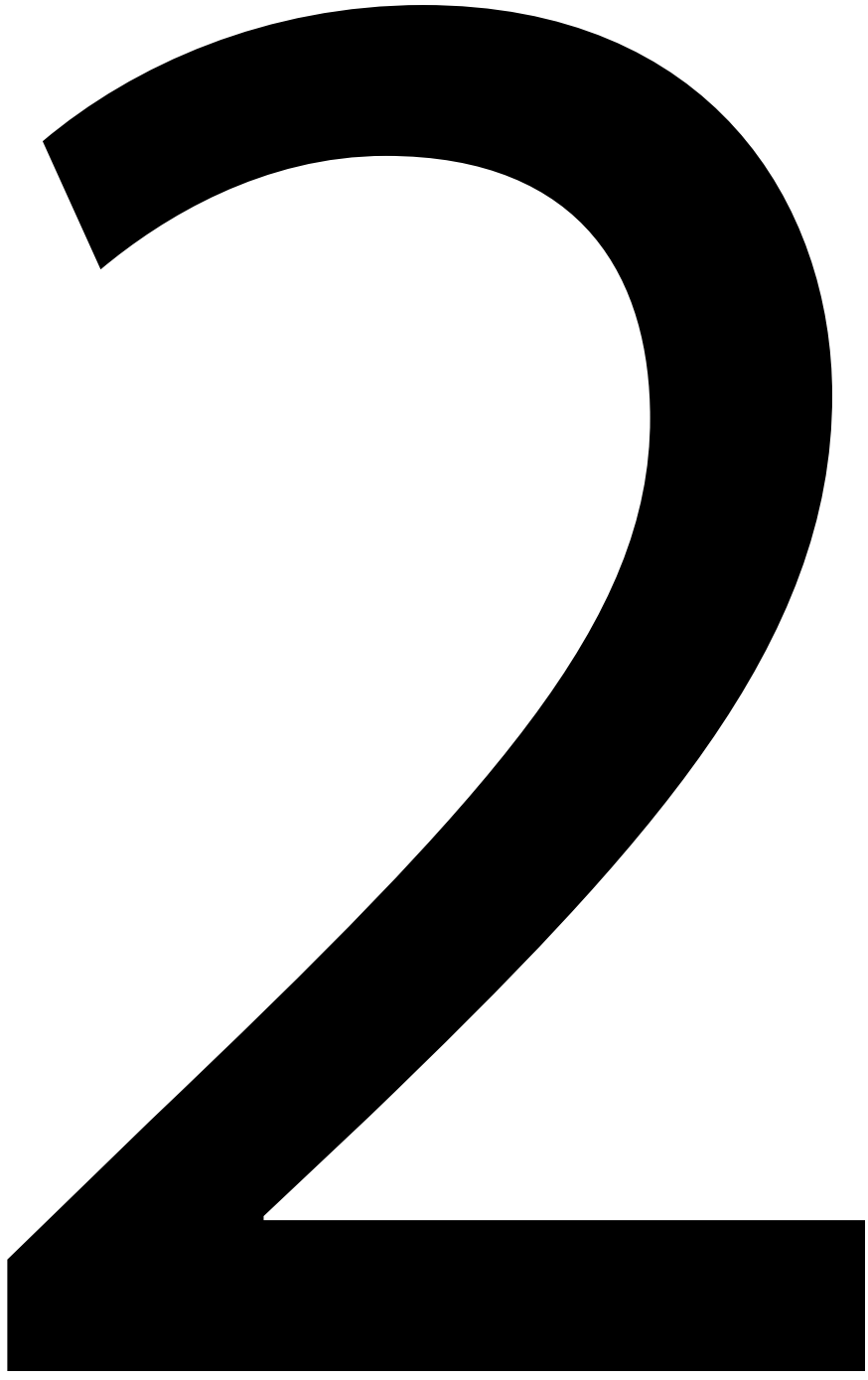

Chapter 2

Autophagy promotes survival in aging submerged cultures of the filamentous fungus *Aspergillus niger*

Benjamin M. Nitsche[1,2,3,*], Anne-Marie Burggraaf-van Welzen[1,3,4,*], Gerda Lamers[1], Vera Meyer[2] and Arthur F.J. Ram[1,3,4]

[1] Molecular Microbiology and Biotechnology, Institute of Biology Leiden, Leiden University, Sylviusweg 72, 2333 BE Leiden, The Netherlands

[2] Applied and Molecular Microbiology, Institute of Biotechnology, Berlin University of Technology, Gustav-Meyer-Allee 25, 13355 Berlin, Germany

[3] Kluyver Centre for Genomics of Industrial Fermentation, P.O. Box 5057, 2600 GA Delft, The Netherlands

[4] Netherlands Consortium for Systems Biology, P.O. box 94215, 1090 GE Amsterdam, The Netherlands

[*] Both authors equally contributed to the manuscript

Appl Microbiol Biotechnol (2013) 97: 8205–8218

Abstract

Autophagy is a well conserved catabolic process constitutively active in eukaryotes that is involved in maintaining cellular homeostasis by targeting of cytoplasmic content and organelles to vacuoles. Autophagy is strongly induced by limitation of nutrients including carbon, nitrogen and oxygen and is clearly associated with cell death. It has been demonstrated that the accumulation of empty hyphal compartments and cryptic growth in carbon starved submerged cultures of the filamentous fungus *Aspergillus niger* is accompanied by a joint transcriptional induction of autophagy genes (Nitsche 2012). This study examines the role of autophagy by deleting the *atg1*, *atg8* and *atg17* orthologs in *A. niger* and phenotypically analyzing the deletion mutants in surface and submerged cultures. The results indicate that *atg1* and *atg8* are essential for efficient autophagy, whereas deletion of *atg17* has little to no effect on autophagy in *A. niger*. Depending on the kind of oxidative stress confronted with, autophagy deficiency renders *A. niger* either more resistant (menadione) or more sensitive (H_2O_2) to oxidative stress. Fluorescence microscopy showed that mitochondrial turnover upon carbon depletion in submerged cultures is severely blocked in autophagy impaired *A. niger* mutants. Furthermore, automated image analysis demonstrated that autophagy promotes survival in maintained carbon starved cultures of *A. niger*. Taken together, the results suggest that besides its function in nutrient recycling, autophagy plays important roles in physiological adaptation by organelle turnover and protection against cell death upon carbon depletion in submerged cultures.

Introduction

The filamentous fungus *Aspergillus niger* is an economically important and versatile cell factory commonly exploited for the industrial-scale production of a wide range of enzymes and organic acids (Archer, 2000; Pel *et al.*, 2007; Andersen *et al.*, 2011). Although numerous studies have been conducted aiming at improving our knowledge of catabolic cellular activities that determine product yields in *A. niger* including secretion of proteases and the unfolded protein response (Mattern *et al.*, 1992; Peberdy, 1994; MacKenzie *et al.*, 2005; Braaksma *et al.*, 2009; Carvalho *et al.*, 2012), the possible role of autophagy in relation to protein production has yet not been studied in *A. niger*.

Autophagy is an intracellular degradation process functioning in the delivery of cytoplasmic proteins and organelles to vacuoles for macromolecule turnover and recycling (Inoue and Klionsky, 2010; Bartoszewska and Kiel, 2011). During autophagy, cellular components are sequestered and transported to lytic compartments in double-membrane vesicles, termed autophagosomes. The outer membrane of the autophagosome fuses with the vacuolar membrane, whereupon a single membrane vesicle is released into the lumen. Following lysis of the autophagic membrane and degradation of its contents by hydrolytic enzymes, the breakdown products are transported back into the cytoplasm for reuse by the cell.

This pathway is highly conserved from yeast to higher eukaryotes and is tightly regulated (Bartoszewska and Kiel, 2011). To date, more than 30 autophagy-related (*atg*) genes have been identified for *Saccharomyces cerevisiae* and other fungi (Xie and Klionsky, 2007; Kanki *et al.*, 2011). One key player controlling the levels of autophagy is the autophagy-related protein Atg1, which is a serine/threonine protein kinase (Inoue and Klionsky, 2010; Bartoszewska and Kiel, 2011). Upon induction of autophagy, this kinase interacts with Atg17, Atg29 and Atg31 in an Atg13-dependent manner, forming the Atg1-kinase complex that initiates the formation of autophagosomes (Kabeya *et al.*, 2005; Cheong *et al.*, 2008) (Cheong 2008; Kabeya 2005). Deletion of the *atg1* ortholog in *Podospora anserina* abolished autophagy and caused several developmental defects (Pinan-Lucarré *et al.*, 2005). Mutants displayed fewer aerial hyphae and did not form protoperithecia. Similar phenotypic traits were observed in *P. anserina* Δ*atg8* mutants (Pinan-Lucarré *et al.*, 2005). Atg8 is coupled to the membrane lipid phosphatidylethanolamine (PE) forming an essential component of autophagic vesicle membranes (Inoue and Klionsky, 2010; Bartoszewska and Kiel, 2011). The *atg8* gene has also been deleted in the filamentous fungus *A. oryzae* resulting in mutants that were defective in autophagy and did not form aerial hyphae conidia (Kikuma *et al.*, 2006).

Autophagy plays an important role in cellular homeostasis by efficient removal of damaged organelles. For filamentous fungi it has been shown that endogenous recycling of cellular

products by autophagy facilitates foraging of hyphae and fuels conidiation under nutrient starvation (Shoji *et al.*, 2006; Richie *et al.*, 2007; Shoji and Craven, 2011). The hyphae that are formed during this starvation-induced (cryptic) re-growth show fewer new branches and significantly decreased diameters (Pollack *et al.*, 2008). In the older portions of the mycelium vacuolation increases dramatically following starvation, resulting in fragmentation and eventually dying of the hyphae.

It has been shown that the morphological response to carbon starvation in submerged batch cultures of the filamentous fungus *A. niger*, including emergence of empty hyphal ghosts and (cryptic) outgrowth of thinner non-branching hyphae, is accompanied by a concerted induction of genes related to autophagy (Nitsche *et al.*, 2012). To gain insights into the function of autophagy during submerged carbon starvation, *A. niger* autophagy mutants were generated by deletion of *atg1*, *atg8* and *atg17* orthologs. The mutants were phenotypically characterized during growth in surface and submerged cultures applying nutrient limitation and oxidative stress. Cytological effects of autophagy deficiency were assessed by investigation of fluorescent reporter strains allowing the visualization of cytoplasm, vacuoles and mitochondria. The results indicate that autophagy plays important roles in the metabolic adaptation to carbon starvation in submerged cultures and promotes the survival of hyphae formed before depletion of the carbon source.

Materials and Methods

Strains, media and molecular techniques

Aspergillus strains used (see Table 1) were grown at 30°C on solidified (20 $g \cdot l^{-1}$ agar) nitrate minimal medium (MM) (Bennett and Lasure, 1991) or complete medium (CM) containing 0.5% (w/v) yeast extract and 0.1% (w/v) casamino acids in addition to MM. The pH of synthetic medium for bioreactor cultivations was adjusted to 3 and contained per liter: 4.5 g NH_4Cl, 1.5 g KH_2PO_4, 0.5 g KCl, 0.5 g $MgSO_4 \cdot 7H_2O$ and 1 ml trace metal solution modified from Vishniac and Santer (1957). After autoclaving, the synthetic medium was supplemented with filter-sterilized 10% (w/v) yeast extract and autoclaved 50% (w/v) glucose solutions to give final concentrations of 0.003% (w/v) and 0.8% (w/v), respectively.

All cloning steps were performed according to the methods described by Sambrook and Russell (2001) using *Escherichia coli* strain DH5α. Transformation of *A. niger* was performed as previously described (Meyer *et al.*, 2010). Hygromycin resistant transformants were isolated from plates supplemented with 200 $\mu g \cdot ml^{-1}$ hygromycin and 50 $\mu g \cdot ml^{-1}$ caffeine and subsequently purified on plates with 100 $\mu g \cdot ml^{-1}$ hygromycin. Phleomycin resistant transformants were isolated and purified on plates supplemented with 100 $\mu g \cdot ml^{-1}$ phleomycin. Southern analysis was performed as described by Sambrook and Russell (2001)

Table 1 | *Aspergillus* strains used in this study

Strain name[1]	Genotype	Source
A. niger		
N402 (ATCC 64974)	*cspA1*	Bos *et al.* (1988)
AB4.1 (ATCC 62590)	*cspA1*, *pyrG*$^-$	van Hartingsveldt *et al.* (1987)
BN30.2 (FGSC A1871)	N402, Δ*atg1*::*hyg*^{R}	This study
BN29.3 (FGSC A1872)	N402, Δ*atg8*::*hyg*^{R}	This study
BN32.2 (FGSC A1873)	N402, Δ*atg17*::*hyg*^{R}	This study
BN38.9 (FGSC A1874)	AB4.1, P*gpdA*::*N-citA*::*gfp*, *pyrG*$^+$	This study
BN39.2 (FGSC A1875)	BN38.9, Δ*atg1*::*hyg*^{R}	This study
BN40.8 (FGSC A1876)	BN38.9, Δ*atg8*::*hyg*^{R}	This study
AW20.10 (FGSC A1877)	BN38.9, Δ*atg17*::*hyg*^{R}	This study
BN56.2 (FGSC A1878)	BN30.2, P*gpdA*::*gfp*, *phl*^{R}	This study
BN57.1 (FGSC A1879)	BN29.3, P*gpdA*::*gfp*, *phl*^{R}	This study
BN58.1 (FGSC A1880)	BN32.2, P*gpdA*::*gfp*, *phl*^{R}	This study
AR19#1 (FGSC A1881)	AB4.1, P*gpdA*::*gfp*, *pyrG*$^+$	Vinck *et al.* (2005)
AW24.2 (FGSC A1882)	BN56.2 , *atg1*, *amdS*$^+$	This study
AW25.1 (FGSC A1883)	BN57.1, *atg8*, *amdS*$^+$	This study
AW26.1 (FGSC A1884)	BN58.1, *atg17*, *amdS*$^+$	This study
A. nidulans		
SRS29	SRF200 (ATCC 200171 x FGSC 851), P*gpdA*::*NcitA*::*gfp*	Suelmann and Fischer (2000)

[1] Accession numbers for public strain repositories are indicated in brackets

using either [α-32P]dATP labeled probes synthesized with the Rediprime II DNA labelling System (Amersham Pharmacia Biotech) or DIG labeled probes generated by PCR with the PCR DIG Probe Synthesis Kit (Roche Applied Science). MM for sensitivity plate assays was solidified with 2% (w/v) agar and supplemented with H_2O_2 or menadione as indicated.

Construction of strains

The vector for constitutive expression of mitochondrially targeted GFP was constructed as follows. A 1.1 kb *NcitA*::*gfp* fragment was PCR amplified from genomic DNA of the *A. nidulans* strain SRS29 (Suelmann 2000), blunt-end ligated into pJET1.2 (Fermentas) and sequenced. Subsequently, the fragment was excised using *Bgl*II and *BamH*I restriction enzymes and ligated into the 3.5 kb *Bgl*II-*BamH*I backbone of pAN52-1N (GenBank: Z32697.1). Next, a 2.2 kb *Bgl*II-*Nco*I P*gdpA* fragment isolated from pAN52-1N was inserted into the *Bgl*II-*Nco*I opened intermediate construct. Finally, a 3.9 kb *Xba*I *pyrG** fragment was isolated from pAB94 (Van Gorcom 1988) and inserted at the *Xba*I site to give the final construct: *PgpdA-NcitA*::*gfp-TtrpC-pyrG**, which was transformed to *A. niger* strain AB4.1 (Hartingsveldt 1987). Single copy integration at the *pyrG* locus was confirmed by Southern analysis according to

the method previously described (Meyer *et al.*, 2010) (see Figure S1). The strain was named BN38.9.

Constructs for gene replacements with the hygromycin resistance cassette were generated as follows. Approximately 1 kb flanking regions of the *atg1* (An04g03950), *atg8* (An07g10020) and *atg17* (An02g04820) open reading frames were PCR amplified from genomic DNA of the N402 wild-type strain using primer pairs according to Table S1, blunt-end ligated into pJET1.2 (Fermentas) and sequenced. Flanks were isolated from the pJET1.2 vectors using enzymes cutting at the outermost restriction sites (as indicated in Table S1) and three-way ligated into a *Not*I-*Kpn*I opened pBluescript II SK(+) vector (Fermentas). For finalizing the *atg1* and *atg17* deletion constructs, the hygromycin resistance cassette was isolated as *Nhe*I-*Xba*I fragment and ligated between the flanking regions within the corresponding intermediate pBluescript constructs. For insertion of the hygromycin resistance cassette between the *atg8* flanks, *Xho*I and *Xba*I were used accordingly. Linearized *atg1*, *atg8* and *atg17* deletion cassettes were transformed to *A. niger* strain N402 and homologous integration was confirmed by Southern analysis (see Figure S2) giving the stains BN30.2, BN29.3 and BN32.2, respectively (see Table 1).

For constitutive expression of cytosolically targeted GFP in the autophagy deletion mutants, the vector pGPDGFP (Lagopodi *et al.*, 2002) was co-transformed with pAN8.1 (Mattern *et al.*, 1988) to *A. niger* strains BN30.2, BN29.3 and BN32.2 (see Table 1). Positive transformants were isolated by screening for cytosolic fluorescence and named BN56.2, BN57.1 and BN58.1, respectively (see Table 1). For complementation of the autophagy deletion strains BN56.2, BN57.1 and BN58.1, the corresponding open reading frames and approximately 1 kb flanking regions were PCR amplified using genomic DNA of the N402 wild-type strain as template and primer pairs as indicated in Table S1. The individual fragments were blunt-end ligated into pJET1.2 and sequenced. Subsequently, the *amdS* cassette was PCR amplified from the *mnsA* deletion construct described by Carvalho *et al.* (2011a) using primers indicated in Table S1, blunt-end ligated into pJet1.2 and sequenced. Subsequently, the *amdS* cassette was isolated as an *Xho*I-*Hind*III fragment and ligated into pBluescript II SK(+). The amplified autophagy gene loci were isolated from the intermediate pJET1.2 vectors via *Not*I digestion and ligated into pBluescript II SK(+) harbouring the *amdS* cassette. The resulting plasmids were transformed to *A. niger* strains BN56.2, BN57.1 and BN58.1, respectively. Random integration of the constructs was confirmed by Southern analysis (Figure S4) and the resulting strains were named AW24.2, AW25.1 and AW26.1 (Table 1).

Deletion of *atg1*, *atg8* and *atg17* in the strain expressing the mitochondrial targeted GFP was performed by transforming linearized *atg1*, *atg8* and *atg17* deletion constructs to *A. niger* strain BN38.9. Homologous integration of the constructs at their respective loci

was confirmed by Southern analysis (see Figure S3) and the resulting strains were named BN39.2, BN40.8 and AW20.10, respectively (Table 1).

Bioreactor cultivation and sampling

Bioreactor cultivations were performed as previously described by Jørgensen *et al.* (2010). Briefly, autoclaved 6.6 L bioreactor vessels (BioFlo3000, New Brunswick Scientific) holding 5 L sterile synthetic medium were inoculated with $5 \cdot 10^9$ conidia. During cultivation, the temperature was set to 30°C and pH 3 was maintained by addition of titrants (2 M NaOH, 1 M HCl). The supply of sterile air was set to 1 $l \cdot min^{-1}$. To avoid loss of hydrophobic spores through the exhaust gas, the stirrer speed was set to 250 rpm and air was supplied via the head space during the first six hours of cultivation. After this initial germination phase, the stirrer speed was increased to 750 rpm, air was supplied via the sparger and 0.01% polypropylene glycol (PPG) P2000 was added to prevent foaming. O_2 and CO_2 partial pressures of the exhaust gas were analyzed with a Xentra 4100C analyzer (Servomex BV, Netherlands). Dissolved oxygen tension (DOT) and pH were measured electrochemically with autoclavable sensors (Mettler Toledo). At regular intervals, samples were taken from the cultures. Aliquots for microscopic analysis were either directly analyzed (fluorescence microscopy) or quickly frozen in liquid nitrogen (automated image analysis), the remainder of the samples was vacuum filtrated using glass microfiber filters (Whatmann). Retained biomass and filtrates were directly frozen in liquid nitrogen and stored at -80°C. Biomass concentrations were gravimetrically determined from freeze dried mycelium of a known mass of culture broth.

Microscopic and image analysis

For the analysis of hyphal diameters, microscopic samples were slowly defrosted on ice and subsequently fixed and stained in a single step by mixing them at a 1:1 ratio with Lactophenolblue solution (Fluka). Per sample, a minimum of 40 micrographs were taken using a 40x objective and an ICC50 camera (Leica). The microscope and camera settings were optimized to obtain micrographs with strong contrast. To measure hyphal diameters in an automated manner, a previously developed macro (Nitsche 2012) for the open source program ImageJ (Abràmoff 2004) was used. DIC and fluorescence images were taken with a Zeiss axioplan 2 imaging microscope equipped with DIC optics. For the GFP settings, an epi-fluorescence filter cubeXF 100-2 with excitation 450-500 nm and emission 510-560 nm was used. Confocal images were obtained using a Zeiss Observer microscope equipped with a LSM 5 exciter. Excitation in the GFP settings was achieved with a 488 Argon laser line with emission 505-550 nm.

Results

Autophagy-related genes *atg1* and *atg8* but not *atg17* are essential for efficient autophagy in *A. niger*

To study the phenotypes of autophagy deficient *A. niger* mutants in surface and submerged cultures, orthologs of three genes known to encode essential components of the autophagic machinery in *S. cerevisae* (Tsukada and Ohsumi, 1993; Matsuura *et al.*, 1997; Kabeya *et al.*, 2005; Cheong *et al.*, 2005) were identified and deleted in *A. niger*. Two of the target genes encode proteins that are part of the regulatory Atg1 kinase complex, namely the kinase Atg1 itself and the scaffold protein Atg17. The third target gene encodes the ubiquitin-like protein Atg8, which is a structural component required for the formation of autophagosomal membranes. The following ortholog pairs were identified by reciprocal best BlastP hit analysis *Scatg1*/An04g03950 ($E=4e^{-151}$), *Scatg8*/An07g10020 $E=4e^{-67}$) and *Scatg17*/An02g04820 ($E=4e^{-12}$), which correspond to those suggested at the Aspergillus Genome Database (Arnaud 2010; Arnaud 2012). The identified target genes were deleted in the *A. niger* laboratory wild-type strain N402 by replacement with a hygromycin resistance cassette. Gene deletions were confirmed by Southern analysis (see Figure S2) and the selected strains were named BN30.2 (Δ*atg1*), BN29.3 (Δ*atg8*) and BN32.2 (Δ*atg17*), and listed in Table 1.

Studies in *A. oryzae* (Kikuma *et al.*, 2006) and *Penicillium chrysogenum* (Bartoszewska and Kiel, 2011) have demonstrated localization of cytosolic fluorescent proteins to vacuoles under starvation conditions in wild-type strains, whereas mutants impaired in autophagy did not show vacuolar localization of cytosolic GFP. In order to assess whether deletion of the selected target genes impairs autophagy in *A. niger*, the Δ*atg1*, Δ*atg8* and Δ*atg17* strains were transformed with a P*gpdA*-GFP construct to obtain the corresponding mutant strains BN56.2, BN57.1 and BN58.1 (see Table 1) with constitutive expression of cytosolic GFP. Vacuolar localization of cytosolic GFP was observed for the wild-type strain during nutrient limitation, while both Δ*atg1* and Δ*atg8* mutants did not show GFP fluorescence inside vacuoles, indicating deficient autophagy. Interestingly, deletion of *atg17* did not affect vacuolar localization of cytosolic GFP (see Figure 1). Complementation studies showed that vacuolar localization of cytosolic GFP during starvation could be restored in the *atg1* and *atg8* complemented mutants (strains AW24.2 and AW25.1, respectively), demonstrating that the described phenotypes of strains BN56.2 and BN57.1 were caused only by the deletion of the *atg1* and *atg8* genes, respectively (see Figure 1). Together, these results suggest that both *atg1* and *atg8* but not *atg17* are essential for efficient autophagy in *A. niger*.

To monitor autophagy mediated turnover of mitochondria, also referred to as mitophagy (Kanki *et al.*, 2011), induced by carbon starvation, wild-type and *atg* deletion strains with constitutive expression of mitochondrially targeted GFP (see Table 1) were generated.

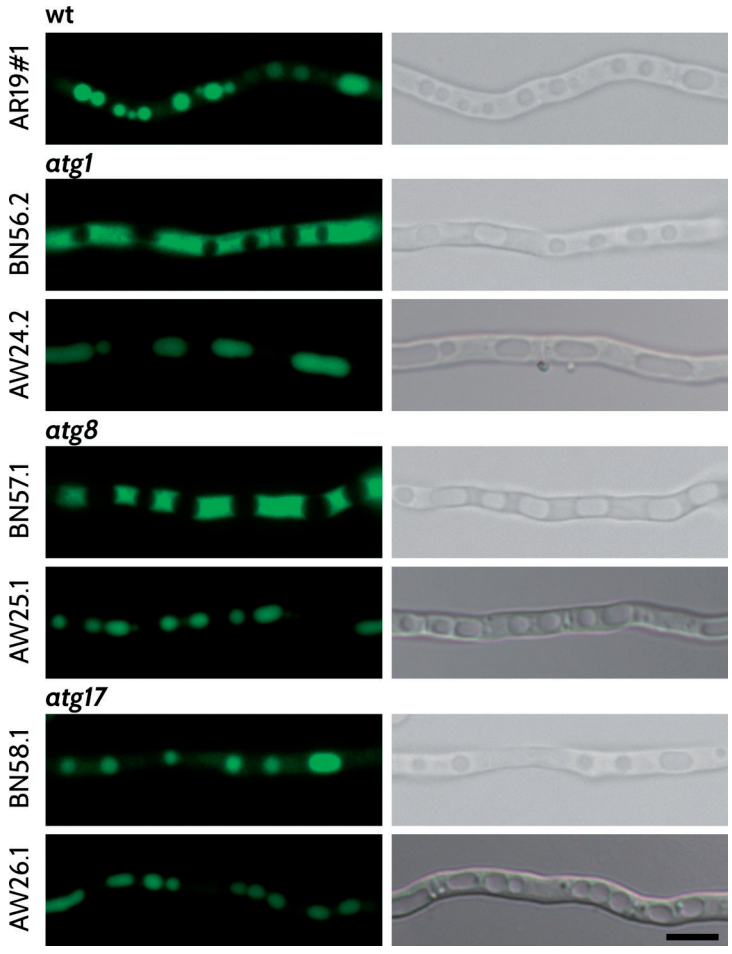

Figure 1 | Localization of cytosolically expressed GFP during carbon starvation. The strains were pre-grown for 8 hours at 30°C on coverslips in Petridishes with liquid MM. Subsequently, coverslips with adherent hyphae were washed and transferred to MM without carbon source. Micrographs were taken 40 hours after transfer. Wild-type (strain AR19#1) and the Δ*atg17* mutant (strain BN58.1) showed vacuolar localization of GFP, whereas both Δ*atg1* and Δ*atg8* mutants (strains BN56.2 and BN57.1, respectively) showed cytosolic localization. Complementation with the corresponding wild-type loci restored vacuolar localization of GFP for the Δ*atg1* and Δ*atg8* mutants (strains AW24.2 and AW25.1, respectively). The phenotype of the complemented Δ*atg17* mutant (strain AW26.1) corresponds to that of the non-complemented strain BN58.1. Scale bar: 5 µm.

The approach described by Suelmann and Fischer (2000), who showed that N-terminal fusion of the mitochondrial targeting sequence from the citrate synthase A to a fluorescent protein efficiently labeled mitochondria in *A. nidulans*, was followed for visualization of mitochondria. Similar to *A. nidulans*, wild-type (strain BN38.9) and *atg* mutant reporter strains (strains BN39.2, BN40.8 and AW20.10) showed fluorescent tubular structures inside hyphae under nutrient rich conditions (data not shown). During carbon starvation however,

microscopic analysis indicated considerable differences in mitochondrial morphology (see Figure 2). The phenotypes correspond to those observed for the localization of cytosolically targeted GFP (see Figure 1). Localization of GFP remained mitochondrial in both Δ*atg1* and Δ*atg8* strains (strains BN39.2 and BN40.8, respectively) upon starvation, whereas wild-type and Δ*atg17* strains (strains BN38.9 and AW20.10, respectively) showed vacuolar localization of mitochondrially expressed GFP. These results show that mitochondrial turnover induced by carbon starvation is mediated by autophagy, which is severely impaired in *A. niger* upon deletion of either *atg1* or *atg8* but not *atg17*.

Phenotypes of Δ*atg1*, Δ*atg8* and Δ*atg17* strains in surface cultures

Depending on which species of filamentous fungi is studied and which *atg* gene is under investigation, defective autophagy results in complete or severe impairment of conidiation during surface growth (Kikuma *et al.*, 2006; Richie *et al.*, 2007; Bartoszewska and Kiel, 2011). To test whether conidiation is affected as well in the Δ*atg1*, Δ*atg8 and* Δ*atg17* mutants (strains BN30.2, BN29.3 and BN32.2, respectively), conidia from colonies grown for 7 days

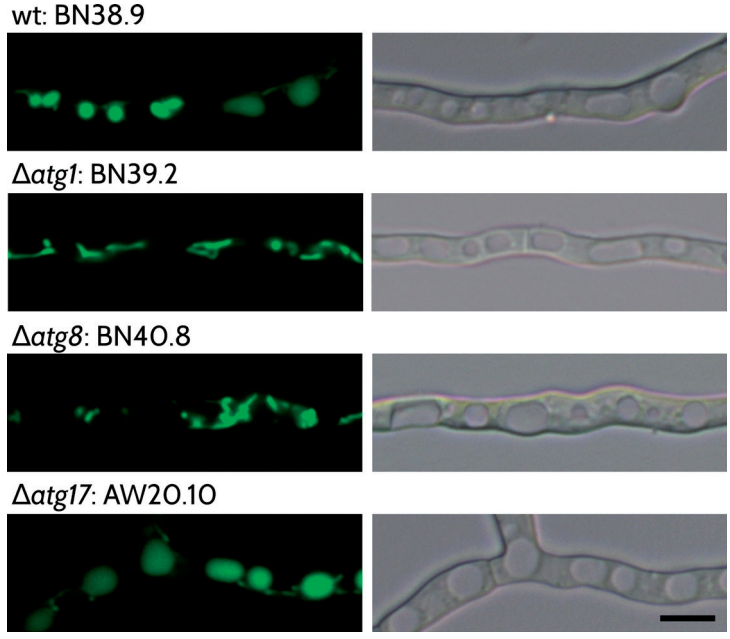

Figure 2 | Localization of mitochondrially expressed GFP during carbon starvation. The strains were grown as described in Figure 1. Wild-type (strain BN38.9) and Δ*atg17* mutant (strain AW20.10) showed vacuolar localization of mitochondrially targeted GFP upon carbon starvation, whereas both Δ*atg1* and Δ*atg8* mutants (strains BN39.2 and BN40.8, respectively) showed cytosolic localization. Under nutrient-rich conditions, all strains showed fluorescent signals resembling tubular mitochondrial networks as described by Suelmann and Fischer (2000) (data not shown). Scale bar: 5 µm.

on solid MM were harvested and counted. Although colonies of the Δ*atg1* and Δ*atg8* strains developed conidiophores and turned dark, the colonies showed slightly attenuated pigmentation (see Figure 3A) indicating reduced spore densities and/or differences in melanization of spores. Indeed, the amount of spores recovered from the colonies was significantly reduced (see Figure 3C). Conidiation was most affected in the Δ*atg8* strain, with a decrease of 70%. Interestingly, although deletion of *atg17* did not repress vacuolar localization of either cytosolic GFP (see Figure 1) or mitochondrial GFP (see Figure 2) under carbon starvation, and its colony appearance was indistinguishable from that of the wild-type, the amount of recovered conidia was reduced by more than 20%. This thus suggests an intermediate phenotype for the deletion of *atg17* in *A. niger*. In agreement to studies in *A. oryzae* (Kikuma *et al.*, 2006), colonies of the Δ*atg8* strain showed slower radial growth on MM (see Figure 3B). Even after correcting for this difference in colony size, conidiation was most reduced for the Δ*atg8* strain as shown by the spore densities (see Figure 3C). However, compared to the *A. oryzae* Δ*atg8* mutant, which was reported not to develop aerial hyphae and conidia (Kikuma *et al.*, 2006), the conidiation phenotype in *A. niger* is much less pronounced.

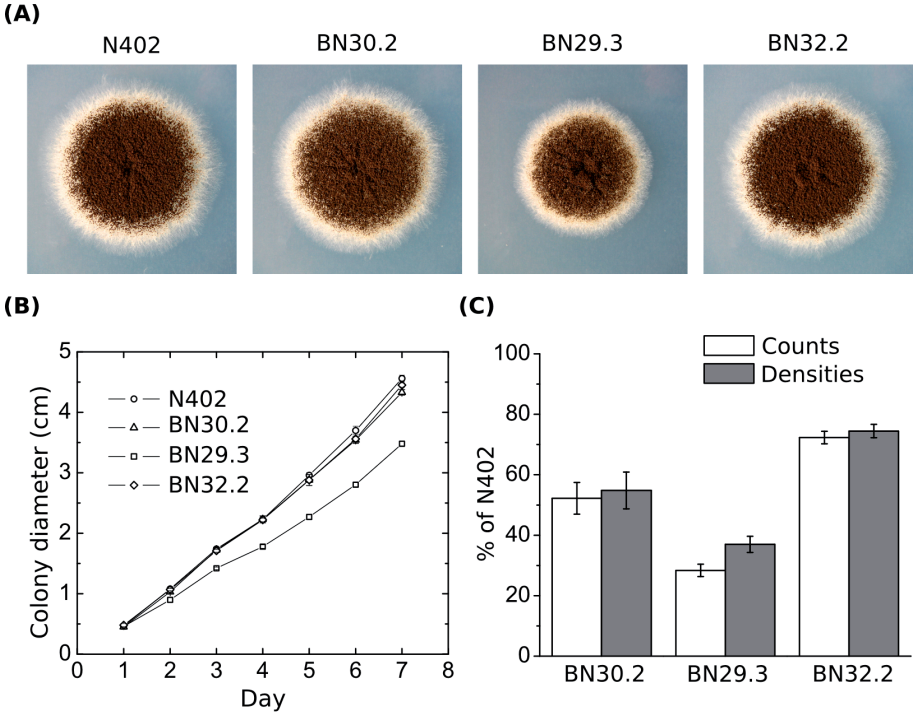

Figure 3 | Conidiation and colony expansion. Wild-type (strain N402) and the Δ*atg1*, Δ*atg8* and Δ*atg17* mutants (strains BN30.2, BN29.3 and BN32.2, respectively) were grown for 7 days on solid MM at 30°C. (A) Colony appearance; (B) Colony diameters (n=3); (C) Recovered conidia (n=3) including spore densities corresponding to spore counts corrected for the colony area.

In filamentous fungi, autophagy has been suggested to contribute to nutrient recycling along the mycelial network promoting foraging of individual substrate exploring hyphae and conidial development (Shoji *et al.*, 2006; Richie *et al.*, 2007; Shoji and Craven, 2011). To elucidate the role of autophagy in nutrient recycling in *A. niger*, the phenotypes of Δ*atg1*, Δ*atg8* and Δ*atg17* strains (strains BN30.2, BN29.3 and BN32.2, respectively) were investigated in comparison to the wild-type under nitrogen and carbon limitation on solid MM (see Figure 4A). The Δ*atg1* and Δ*atg8* strains were clearly more affected by nutrient limitation than the wild-type as shown by their strong conidiation phenotypes. The Δ*atg8* strain was more sensitive to nitrogen limitation than the Δ*atg1* strain, whereas both deletion strains were comparably affected by carbon limitation. Figure S5 shows that these phenotypes induced by carbon and nitrogen limitation could be restored through complementation with the corresponding wild-type *atg* loci. In accordance with results shown in Figures 1, 2 and 3A, deletion of *atg17* results in a phenotype that is indistinguishable from that of the wild-type strain N402.

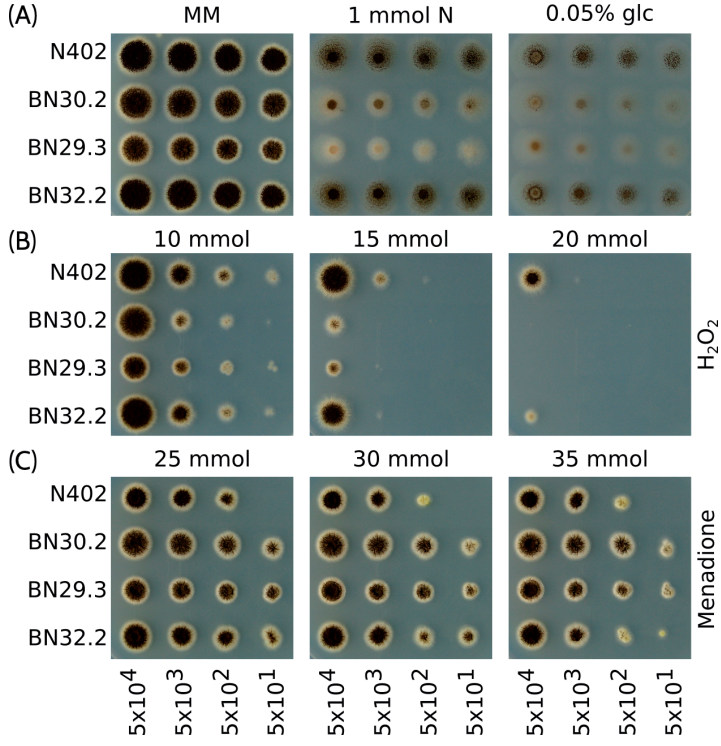

Figure 4 | Sensitivity assay of Δ*atg1*, Δ*atg8*, Δ*atg17* and wild-type strains (strains BN30.2, BN29.3, BN32.2 and N402, respectively). 10-fold dilutions ($5{\cdot}10^4$–50 conidia) were spotted on plates with (A) MM and MM with N (nitrate) or C (glucose) limitation as well as MM supplemented with (B) H_2O_2 or (C) menadione. Plates were incubated for 4 days at 30°C.

In addition to its role in nutrient recycling, numerous reports have shown that autophagy is closely associated with Programmed Cell Death (PCD) (Codogno and Meijer, 2005; Pinan-Lucarré *et al.*, 2005; Veneault-Fourrey *et al.*, 2006). Among the major triggers of PCD are reactive oxygen species (ROS) and the damage they can cause to lipids, carbohydrates, DNA and proteins. Oxidative stress related phenotypes of the Δ*atg1*, Δ*atg8* and Δ*atg17* mutants (strains BN30.2, BN29.3 and BN32.2, respectively) in comparison to the wild-type strain N402 were thus investigated. Sensitivity assays with H_2O_2 and the superoxide anion generator menadione, which have been shown to cause distinct oxidative stress responses in yeast and filamentous fungi (Jamieson, 1992; Thorpe *et al.*, 2004; Tucker and Fields, 2004; Pócsi *et al.*, 2005), are shown in Figure 4B-C. In comparison to the wild-type, all mutants displayed differential phenotypes in response to treatment with the two compounds. Interestingly, H_2O_2 and menadione had opposing effects. The autophagy mutants were more sensitive to H_2O_2, while their resistance to menadione was increased. The Δ*atg17* strain displayed an intermediate phenotype, which was more comparable to that of the wild-type. Complementation studies showed that all described oxidative stress related phenotypes could by partly restored upon expression of the corresponding wild-type gene (Figure S5).

Taken together, the phenotypic characterizations suggest that autophagy is severely impaired in *A. niger* upon deletion of either *atg1* or *atg8*. Contrary to this, deletion of *atg17* showed little to no phenotypic effect when compared to the wild-type. For the subsequent analysis of autophagy impairment during submerged cultivation, the analysis was therefore restricted to the investigation of Δ*atg1* and Δ*atg8* mutants.

Phenotypes of Δ*atg1* and Δ*atg8* strains during submerged growth

It has been demonstrated that the majority of genes related to autophagy show joint transcriptional induction during the post-exponential phase in carbon limited submerged batch cultures of *A. niger* (Nitsche *et al.*, 2012). Concomitantly, old hyphae grown during the exponential phase undergo cell death resulting in an increased fraction of empty hyphal compartments and secondary (cryptic) growth of thin non-branching hyphae. Although it has been shown for filamentous fungi that autophagy plays an important role in nutrient recycling during surface growth (Shoji *et al.*, 2006; Richie *et al.*, 2007; Shoji and Craven, 2011), its function in submerged cultures remains obscure. To gain insights into the role of autophagy during submerged carbon starvation and to investigate how autophagy is related to the phenomena of cell death and secondary growth, Δ*atg1* and Δ*atg8* mutants (strains BN30.2 and BN29.3, respectively) were grown in bioreactors and maintained starving up to six days after carbon depletion (see Figure 5).

The application of bioreactor technology allowed highly reproducible culture conditions. Monitoring of physiological parameters (data not shown) including dissolved oxygen, O_2 and CO_2 partial pressures in the off-gas and titrant (NaOH and HCl) addition, allowed

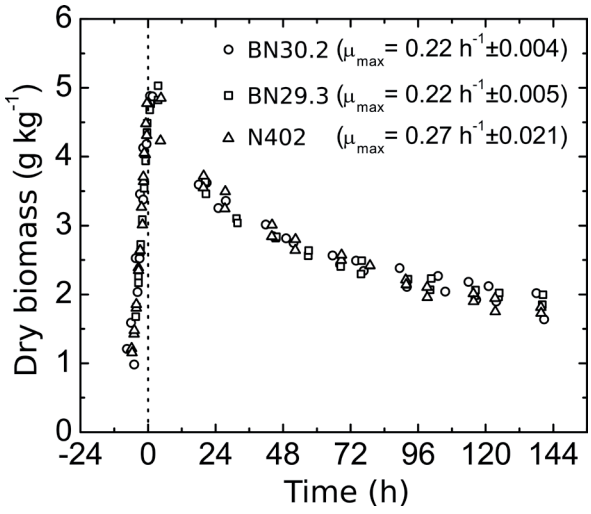

Figure 5 | Carbon starvation in submerged batch cultures. Duplicate biomass profiles of the wild-type (strain N402), the Δ*atg1* and Δ*atg8* mutants (strains BN30.2 and BN29.3, respectively) are shown. The time points of carbon depletion were set to 0 hours and used for synchronization of (replicate) cultures.

synchronization of (replicate) cultures. The described cultivation conditions prevented the formation of mycelial aggregates (pellets) and guaranteed a dispersed macromorphology during all cultivations. Interestingly, in contrast to the colony expansion rates on solid media (see Figure 3A-B), the maximum specific growth rates for both mutants during exponential growth were affected to the same extend. The mutants grew slower (μ_{max}=0.22h^{-1} ± 0.005) than the wild-type (μ_{max}=0.27h^{-1} ± 0.021). The biomass profiles did not show any considerable differences during the post-exponential phase (see Figure 5).

Flow chamber experiments with *A. oryzae* (Pollack *et al.*, 2008) have shown that carbon depletion induces outgrowth of hyphae with strongly reduced diameters. A similar morphological response has been observed during carbon starvation in submerged cultures of *A. niger* (Nitsche *et al.*, 2012). An automated image analysis approach allowed for monitoring of hyphal population dynamics of the cytoplasm filled mycelial fraction and demonstrated a gradual transition from thick (old) to thin (young) hyphae during the post-exponential phase. This transition reflects cell death resulting in the emergence of empty thick compartments fueling secondary (cryptic) regrowth in the form of non-branching thin hyphae. To examine whether autophagy affects this transition dynamics, microscopic pictures of the wild-type, the Δ*atg1* and Δ*atg8* strains from carbon limited bioreactor batch cultures were analyzed accordingly (see Figure 6). During exponential growth (day 0), all three strains displayed single populations of thick hyphae with mean diameters of approximately 2.2 µm. After carbon depletion, populations of thin hyphae with mean diameters of around 1 µm emerged. This transition was gradual for the wild-type,

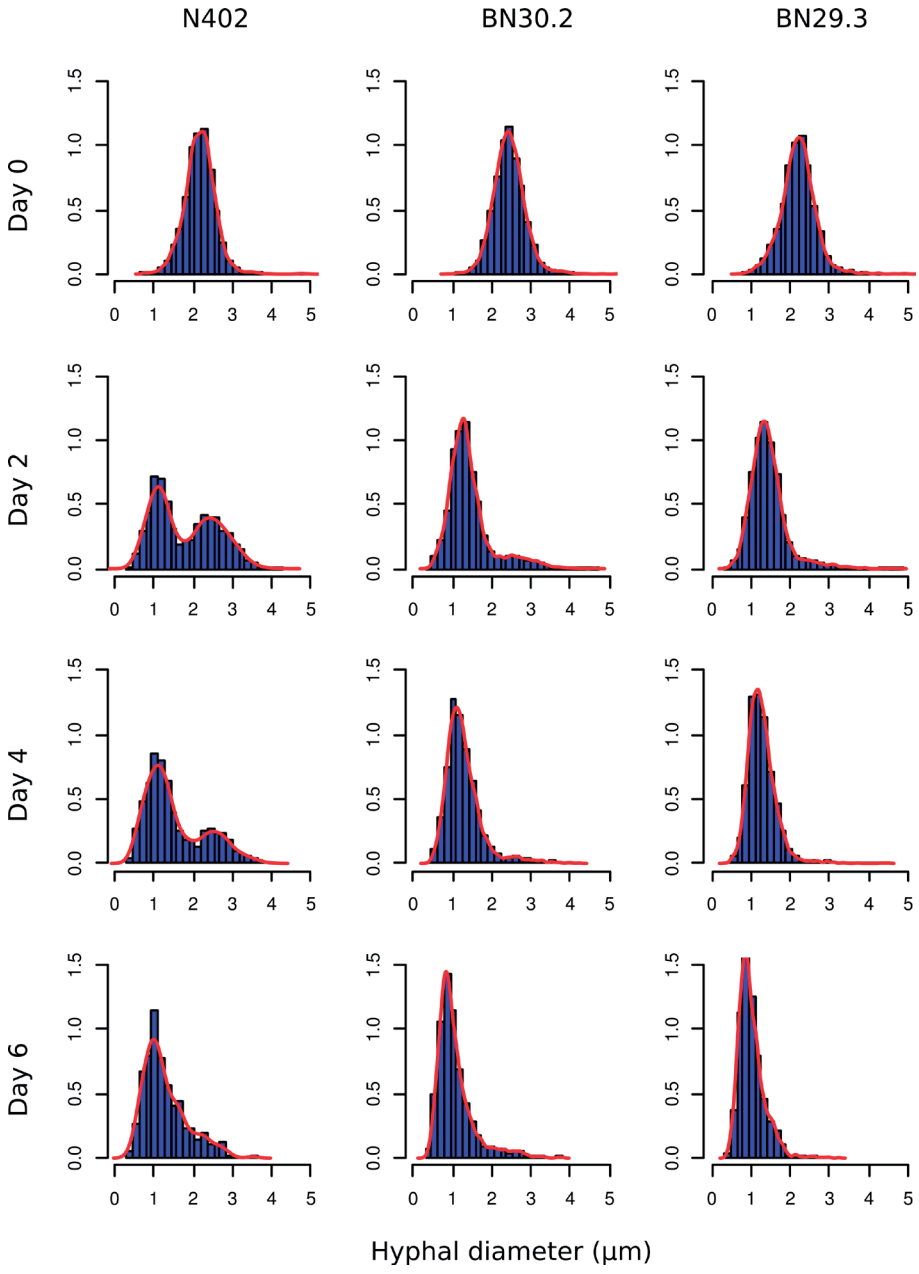

Figure 6 | Hyphal diameter populations. Population dynamics of hyphal diameters for the wild-type (strains N402), the Δ*atg1* and Δ*atg8* mutants (strains BN30.2 and BN29.3, respectively) are shown. Micrographs (≥40) of dispersed hyphae were analyzed by automated image analysis per strain and time point. Day 0 refers to the exponential growth phase, whereas the subsequent three time points refer to 2, 4 and 6 days of carbon starvation.

while it was clearly accelerated for the Δ*atg1* and Δ*atg8* mutants, suggesting enhanced cell death rates for the older mycelium (thick hyphae) upon impairment of autophagy.

It has been shown that autophagy is important for mitochondrial maintenance and degradation of excess mitochondria during the stationary phase of *S. cerevisiae* cultures, which is of outermost importance because mitochondria play a key role in metabolism and cell death signaling (Zhang *et al.*, 2007). In order to monitor whether the degradation of mitochondria in *A. niger* is similarly affected during carbon starvation in submerged cultures, the reporter strains BN38.9 (wild-type), BN39.2 (Δ*atg*1) and BN40.8 (Δ*atg8*) with constitutive expression of mitochondrially targeted GFP (see Figure 2) were cultured in carbon limited bioreactor batch cultures and monitored by fluorescent microscopy. Hyphae from the exponential growth phase showed fluorescent tubular structures resembling those described by Suelmann et al. (2000) and no difference in mitochondrial morphology was observed between the three strains (see Figure 7A). However, clear differences became apparent upon depletion of the carbon source. The mitochondrially targeted GFP was located inside the vacuoles of the wild-type reporter (strain BN38.9), whereas no vacuolar GFP signal was detected for both Δ*atg1* and Δ*atg8* mutants (strains BN39.2 and BN40.8, respectively) as shown in Figure 7B-C. The density of mitochondrial structures decreased in the wild-type hyphae but accumulated in the intervacuolar space for both mutants. Further, there were considerable differences in the mitochondrial morphology. Remaining mitochondrial structures were largely tubular in the wild-type, while they appeared as fragmented and punctuated structures in the mutants.

Discussion

To our knowledge, this is the first published study investigating autophagy in the industrially important filamentous fungus *A. niger*. Improving our understanding of this catabolic pathway and its role during submerged cultivation is of great interest because autophagy has been shown to be involved in endogenous recycling and the regulation of cell death, both of which can have a direct impact on the yield of bioprocesses (Zustiak *et al.*, 2008; Bartoszewska and Kiel, 2011). For different filamentous fungi, several studies have described the phenomena of carbon starved submerged cultures (White *et al.*, 2002; Emri *et al.*, 2004, 2005, 2006). A generic term that has emerged frequently in this context is autolysis. This term has been generally used to describe hallmarks of aging cultures including declining biomass, increasing extracellular ammonia concentration, hyphal fragmentation and increasing extracellular hydrolase activities (White *et al.*, 2002). Considerable effort has been made to analyze extracellular hydrolase activities (McNeil *et al.*, 1998; McIntyre *et al.*, 2000; Emri *et al.*, 2005) as well as developmental mutants differentially affected in aging carbon starved cultures (Emri *et al.*, 2005). However, the role of autophagy in those cultures has not

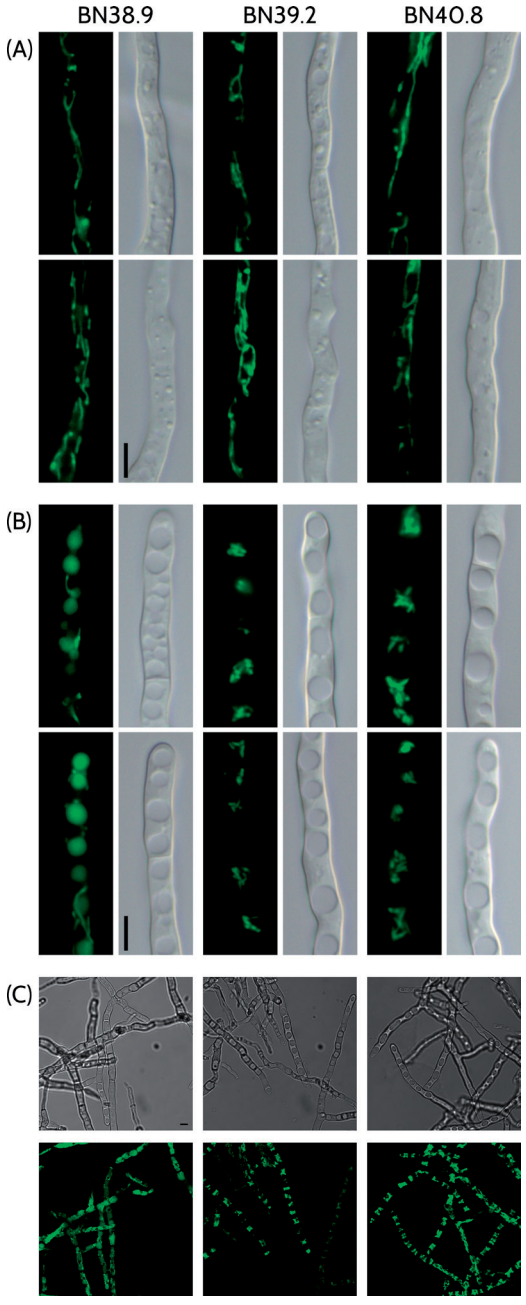

Figure 7 | Localization of mitochondrially targeted GFP during submerged carbon starvation. Constitutive expression of mitochondrially targeted GFP in the wild-type (strain BN38.9), the Δ*atg1* and Δ*atg8* mutants (strains BN39.2 and BN40.8, respectively) during carbon limited batch cultures. Differential interference contrast and fluorescence microscopy of hyphae from (A) the exponential growth phase and (B) 7 hours post-carbon depletion. (C) Confocal laser scanning microscopy of mycelial biomass at 14 hours post-carbon depletion. Scale bars: 5 µm.

attained much attention yet. In a recent systems level analysis of the *A. niger* transcriptome during submerged carbon starvation, autophagy has been identified as a predominantly induced key process (Nitsche *et al.*, 2012). This present study thus aimed at elucidating whether autophagy protects from or promotes loss of hyphal integrity, which was mainly observed by the formation of empty hyphal ghosts.

Two genes encoding components of the regulatory Atg1 kinase complex, namely the genes homologous to the kinase Atg1 itself and the scaffold protein Atg17, were deleted in *A. niger*. In addition, a homolog of the *atg8* gene encoding a membrane protein required for autophagosome formation and extension was deleted in *A. niger*. In agreement to studies in yeast and other filamentous fungi (Bartoszewska and Kiel, 2011), the results demonstrate that deletion of either *atg1* or *atg8* is sufficient to severely impair autophagy in *A. niger*.

However, conflicting with results obtained in *S. cerevisiae* (Kabeya *et al.*, 2005; Cheong *et al.*, 2005), where the absence of Atg17 severely reduces the level of autophagy, deletion of *atg17* in *A. niger* did not show clear phenotypes. Except for a slightly attenuated spore formation (see Figure 3) and intermediate phenotypes in response to oxidative stress (see Figure 4), deletion of *atg17* was indistinguishable from the wild-type. Similarly, the deletion of *atg13* in *A. oryzae* encoding another subunit of the Atg1 kinase complex was reported to only gently affect autophagy, whereas deletion of its counterpart in *S. cerevisiae* clearly impaired it (Kikuma and Kitamoto, 2011). The authors suggested that Atg13 acts as an amplifier resulting in higher autophagic activities in *A. oryzae*. Probably, Atg17 has a similar enhancing role during autophagy induction in *A. niger* leading to the intermediate phenotypes described in this study. However, although the selected *atg17* ortholog (An02g04820) is highly conserved among filamentous fungi, its homology to *Scatg17* is considerably less ($E=4e^{-12}$). Further functional analyses remain to be done to elucidate whether An02g04820 is indeed a functional ortholog of *Scatg17*.

Endogenous recycling of nutrients by autophagy has been supposed to be an important mechanism for nutrient trafficking along the mycelial network promoting foraging of substrate exploring filaments and the formation of aerial hyphae bearing conidiophores (Shoji *et al.*, 2006; Richie *et al.*, 2007; Shoji and Craven, 2011). Similar to studies with other filamentous fungi (Kikuma *et al.*, 2006; Richie *et al.*, 2007; Bartoszewska and Kiel, 2011), impairment of autophagy in *A. niger* considerably reduced conidiation (see Figure 3), a phenotype, which was much enhanced by carbon and nitrogen starvation (see Figure 4A). However, in comparison to other filamentous fungi, this phenotype is much less pronounced, potentially indicating an important difference between *A. niger* and other filamentous fungi including *A. fumigatus* and *A. oryzae*. Alternatively, the explanation could possibly lie in the fact that the *A. niger* wild-type strains used in this study have short conidiophores (*cspA1* mutant background) (Bos *et al.*, 1988) in which conidiophore development might be less

affected because nutrients have to traffic along a shorter distance when condidiophore stalks are short.

In addition to its role in nutrient recycling, autophagy has been shown to be associated with programmed cell death (PCD), which is classically categorized into three types, namely apoptotic (type I), autophagic (type II) and necrotic (type III) cell death. Although autophagy is also referred to as type II PCD, it is not explicitly causative to cell death. Depending on the organism, cell type and stressor, autophagy has been shown to promote both cell death and survival. In filamentous fungi, it has for example been demonstrated to protect against cell death during the heterokaryon incompatibility reaction in *P. anserina* (Pinan-Lucarré *et al.*, 2005) or during carbon starvation in *Ustilago maydis* (Nadal 2010). Contrary to this, autophagy induced cell death is required for rice plant infection by *Magnaporthe grisea* (Veneault-Fourrey *et al.*, 2006). Loss of cellular integrity and subsequent death induced by damage of organelles, macromolecules and membranes through reactive oxygen species (ROS) are a major threat for aerobic organisms. Well described enzymatic and non-enzymatic defense systems have evolved that detoxify ROS (Bai *et al.*, 2003). Autophagy is one of the major pathways for turnover of redundant or damaged organelles and proteins. The described hypersensitivity of autophagy mutants to H_2O_2 could thus be explained by an impaired capability of the mutants to sequester and degrade proteins and organelles damaged by H_2O_2. The increased resistance to menadione however, came at a surprise but might be related to an adaptive stress response in autophagy deficient mutants. In *S. cerevisiae*, it was for example shown that disruption of essential autophagy-related genes results in increased oxidative stress and superoxide dismutase activities (Zhang *et al.*, 2007). Further, adaptive responses to oxidative stress induced by sublethal concentrations of exogenous oxidants have been demonstrated to protect yeast cells against higher lethal concentrations (Jamieson, 1992; Fernandes *et al.*, 2007). Whether an endogenous adaptive mechanism explains the increased menadione resistance of autophagy deficient mutants remains to be shown in future studies.

Hyphal population dynamics showed that the transition from old (thick) to young (thin) hyphae in response to carbon starvation during submerged cultivation was accelerated for both Δ*atg1* and Δ*atg8* mutants when compared to the wild-type (see Figure 6). These results suggest that autophagy protects old mycelium from the exponential growth phase under carbon starvation conditions and delays cell death. Fluorescence microscopy of wild-type, Δ*atg1* and Δ*atg8* reporter strains with GFP-labeled mitochondria revealed that degradation of mitochondria in response to carbon starvation is impaired in autophagy deficient mutants. In yeast, the degradation of excess mitochondria during the stationary phase constitutes a physiological adaptation to the reduced energy requirement of the cells (Kanki *et al.*, 2011). Impairment of autophagy has been shown to lead to mitochondria dysfunction and the accumulation of ROS in yeast stationary phase cultures starved for nitrogen (Suzuki

et al., 2011). It is thus tempting to speculate that autophagy impairment in *A. niger* leads to increasing cellular ROS levels caused by the accumulation of excessive and damaged mitochondria during carbon starvation in submerged cultures, which subsequently causes loss of cellular integrity and finally the emergence of empty hyphal compartments. Taken together, the results indicate that an induction of autophagy upon carbon starvation in submerged cultures of *A. niger* is not exclusively required for endogenous recycling but constitutes an important physiological adaptation by turnover of excessive mitochondria.

Acknowledgements

This work was supported by grants of the SenterNovem IOP Genomics project (IGE07008). It was carried out within the research programme of the Kluyver Centre for Genomics of Industrial Fermentation which is part of the Netherlands Genomics Initiative / Netherlands Organization for Scientific Research. This work was (co)financed by the Netherlands Consortium for Systems Biology (NCSB) which is part of the Netherlands Genomics Initiative / Netherlands Organisation for Scientific Research. We thank Reinhard Fischer from the Karlsruhe Institute of Technology in Germany for providing us with the strain SRS29. We thank Crescel Martis and Leonie Schmerfeld for their technical assistance.